Development 130, 1805-1816

doi:10.1242/dev.00406

A role for actin dynamics in individualization during spermatogenesis in *Drosophila melanogaster*

Tatsuhiko Noguchi* and Kathryn G. Miller

Department of Biology, Washington University in St Louis, Campus Box 1229, 1 Brookings Drive, St Louis, MO 63130, USA
*Author for correspondence (e-mail: noguchi@biology2.wustl.edu)

Accepted 23 January 2003

SUMMARY

In order to better understand the mechanism of sperm individualization during spermatogenesis in *Drosophila melanogaster*, we have developed an in vitro culture system in which we can perform live observation of individualization in isolated cysts. The whole process of individualization, during which a bundle of 64 syncytial spermatids is separated into individual sperm, takes place in these cultures. Individualization complexes, which consist of 64 cones of actin that assemble around the sperm nuclei, move to the basal end of the tails, forming a characteristic 'cystic bulge' that contains an accumulation of cytoplasm, syncytial membrane and vesicles. The cystic bulge is the site of membrane remodeling and its movement was used to follow the progress of individualization. The speed of cystic bulge movement is fairly constant along the length of the cyst. Actin drugs, but not microtubule drugs inhibit cystic bulge movement, suggesting that the movement requires proper actin dynamics but not microtubules. GFP-tagged actin was expressed in the cyst and fluorescence recovery after photobleaching was monitored using confocal microscopy to analyze actin dynamics in cones. Actin turns over throughout the cone, with that at the leading edge of the cones turning over with slightly faster kinetics. Actin does not treadmill from the front to the back of the cone. Actin in moving actin cones turns over in about 12 minutes, although prior to onset of movement, turnover is much slower. Visualization of membrane using FM1-43 reveals that the cystic bulge has an extremely complicated series of membrane invaginations and the transition from syncytial to individualized spermatids occurs at the front of the actin cones. We also suggest that endocytosis and exocytosis might not be important for membrane remodeling. This system should be suitable for analysis of defects in male sterile mutants and for investigating other steps of spermatogenesis.

Movies available online

Key words: Individualization, Spermatogenesis, *Drosophila*, Actin cone, Microtubule, Actin dynamics, Membrane dynamics

INTRODUCTION

During late stages of spermatogenesis in *Drosophila*, a cyst of 64 syncytial spermatids elongates as the sperm axonemes are formed inside it. Then this elongated cyst is remodeled into individual sperm (Fig. 1) by a process called individualization. At the start of individualization actin cones assemble around the spermatid nuclei and then synchronously move from the heads to the tips of the tails (Fabrizio et al., 1998; Lindsley and Tokuyasu, 1980; Tokuyasu et al., 1972). As the actin cones move, a large accumulation of cytoplasm and vesicles, called the cystic bulge, forms around them. In the cystic bulge, the membrane of the cyst is remodeled to enclose each sperm axoneme. Individualization is especially interesting as a cell biological process because it requires an unusual amount of membrane remodeling using a well-defined actin structure. The fully elongated cyst can be up to 1800 μm long (Tokuyasu et al., 1972); therefore, this process requires the actin structures important for the process to move unidirectionally over a significant length. During the process, the bulk of the cytoplasm is discarded from the cell body. However, we have little information about the mechanism of this process.

Drosophila spermatogenesis is an excellent system in which to study the genetic analysis of the differentiation of germ cells from gonial precursor cells to motile sperm, including regulation of germ cell proliferation, meiosis, mitochondoria derivative formation, flagella formation and individualization (Castrillon et al., 1993; Fuller, 1993; Kemphues et al., 1980). A large number of male sterile mutations that affect different aspects of spermatogenesis have been identified (Castrillon et al., 1993; Gonczy et al., 1992; Laughran et al., 1976; Lifschytz and Hareven, 1977; Lindsley and Lifschytz, 1972; Romrell et al., 1972; Wilkinson et al., 1974), and in these collections are mutants that affect individualization specifically (Castrillon et al., 1993; Fabrizio et al., 1998). In addition, the morphological stages of spermatogenesis have been well characterized at the ultrastructural level by electron microscopy (Lindsley and Tokuyasu, 1980; Tokuyasu et al., 1972) (A. D. Tates, PhD Thesis, Rijksuniversitei, Lieden, 1971). Moreover, a few

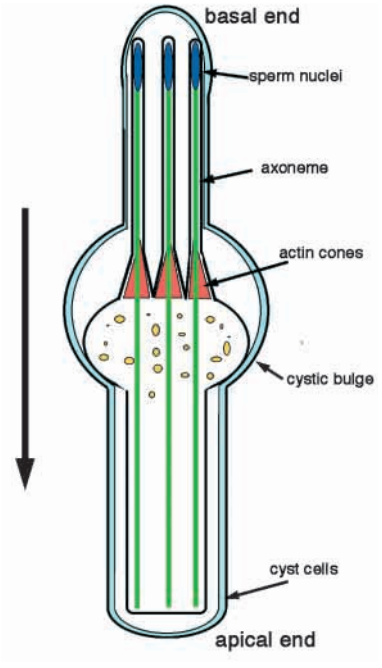

Fig. 1. An individualizing cyst. Individualization takes place at the cystic bulge. The membrane reorganization occurs as the actin cone (red triangle) moves down along the sperm axoneme from its head to the end of the tail. Arrow indicates the direction of movement. Cytoplasm and membranous organelles are squeezed out and accumulate in the cystic bulge as the actin cones move down the cyst. At the end of individualization all cytoplasm and organelles are discarded as a waste bag and 64 thin individual sperm are formed.

previous reports have provided some molecular information about genes involved in individualization [e.g. myosin VI (Hicks et al., 1999) and clathrin (Bazinet et al., 1993; Castrillon et al., 1993; Fabrizio et al., 1998)]. However, despite the large amount of genetic information about some aspects of spermatogenesis, the mechanism of individualization is poorly understood, because of a lack of cell biological information and knowledge of many of the molecules involved.

To provide information on the mechanism, we wanted to be able to manipulate the process and to visualize the events in the cystic bulge at high resolution. For this reason, we developed an in vitro culture system. Previously, it has been demonstrated that isolated spermatogenic cysts of *Drosophila melanogaster* and *Drosophila hydei* undergo differentiation in vitro to some extent (Cross and Shellenbarger, 1979; Fowler, 1973; Liebrich, 1981; Liebrich, 1982). Cross and Shellenbarger (Cross and Shellenbarger, 1979) described meiosis and reported that all subsequent steps of spermatogenesis take place in isolated and cultured cysts of *D. melanogaster*. However, these studies did not investigate the individualization step in detail. This previous work encouraged us to develop the culture system further to permit observation and manipulation of individualizing cysts. We have adapted the culture system so that we can employ advanced live imaging techniques.

The main questions we have asked are: what is the driving force for cystic bulge movement? Are the actin cones responsible for movement? How is the syncytial membrane reorganized into a thin tubular structure? For these studies, we have used immunofluorescence localization of microtubules and F-actin during formation and movement of the actin cones, pharmacological manipulation of cytoskeletal elements and fluorescence recovery after photobleaching (FRAP) techniques to demonstrate that actin dynamics play a key role in the process. In addition, membrane dynamics in the cystic bulge were visualized using FM1-43. Based on these observations, we propose a model for the role of actin in individualization. This is the first detailed description of individualization in vitro and dissection of the cell biological processes involved.

MATERIAL AND METHODS

Drosophila strains and husbandry

D. melanogaster were raised on standard cornmeal at room temperature. Oregon R was used as the wild-type strain. Three drivers line for gene expression (see below) in germline cells in the testis: pCOG-GAL4; NGT-40; nanos-GAL4 (Robinson and Cooley, 1997; Tracey et al., 2000) and pUASpGFP-actin line (Hudson and Cooley, 2002; Rørth, 1998) were kind gifts from Andrew Hudson (Yale University), and *Shibire*^{1} (van der Bliek and Meyerowitz, 1991) was obtained from the Bloomington Stock Center.

Cell culture and live recordings

In vitro culture of isolated cysts was performed according to Cross and Shellenbarger (Cross and Shellenbarger, 1979) with the following modifications. Testes were dissected from newly eclosed adult males and transferred into culture media (modified M3 medium without bicarbonate; Sigma-Aldrich, St Louis, MO), containing 10% fetal calf serum (Sigma-Aldrich) and standard penicilin/streptomycin cocktail (Cross and Sang, 1978; Cross and Shellenbarger, 1979). This formulation supported the best viability and differentiation of isolated cysts, although for observation of individualization, there were no significant differences among the several media we tested (which were based on those used for culturing *Drosophila* cells). The basal end of the testis proximal to the seminal vesicle was cut off using a sharp glass needle, while the apical end of the testis was held using a forceps. Then, the fully elongated cysts were gently squeezed out from the muscle layer of the testis using the side of the glass needle. Isolated cysts were transferred to culture media and cultured at room temperature. This procedure does not damage the cysts and viability tests revealed that 80-90% of the cysts were alive after 24 hours of culture in vitro (data not shown).

In pharmacological experiments, cysts were cultured in 24-well plates (Falcon, Franklin Lakes, NJ) with 1 ml of culture media. The actin depolymerizing drug latrunculin A (LTA, Molecular Probes, Eugene, OR); the actin stabilizing drug jasplakinolide (Molecular Probes); the microtubule depolymerizing drugs colchicine (SIGMA-Aldrich) and nocodazole (SIGMA-Aldrich); the inhibitor of kinesin motor ATPase monastrol (SIGMA-Aldrich); and the myosin ATPase inhibitor 2-3-butanedion monoxime (BDM, SIGMA-Aldrich) were separately dissolved in dimethylsulfoxide (DMSO) for stock solutions. An equal volume of culture media containing twice as much as the final concentration of each drug was added directly to culture media during a recording of the movement of the cystic bulge. Serial differential interference contrasted (DIC) microscope images of the cystic bulge were collected using an inverted microscope equipped with a 10× plan fluor lens (Nikon, Japan) and CCD camera (SPOT, Diagnostic instruments inc. Sterling Heights, MI) every 10 or 12 minutes and processed and plotted using NIH image 1.62 and Microsoft Excel.

Immunofluorescence microscopy and image acquisition

Anti-α-tubulin antibody (DM1A, SIGMA-Aldrich) was used for tubulin staining. Isolated cysts were fixed with 4% paraformaldehyde (EM grade, Electron Microscope Science, PA) in phosphate-buffered saline, pH 7.2 (PBS) for 7 minutes at room temperature. Then cell membranes were extracted by 0.1% Triton X-100 in PBS for 15 minutes. After three washes with PBS, cysts were incubated in blocking solution (2% Bovine serum albumin in PBS) for 1 hour at room temperature. Cysts were kept in 1/300 dilution of primary antibody in blocking solution for 2 hour and washed three times, followed by incubation with secondary antibody (Alexa-488 conjugated goat anti-mouse IgG; Molecular Probes), Alexa 568-

phalloidin (Molecular Probes) and DAPI (SIGMA-Aldrich) for 2 hours. After washing with PBS, cysts were mounted on glass slides with Mowiol (Calbiochem, San Diego, CA). Specimens were examined with an inverted epifluorecscence microscope (ECLIPSE TE200, Nikon, Japan) with a cooled CCD camera (Quantix, Photometrics, Tucson, AZ). The images were deconvolved digitally using Slide book software (Intelligent Imaging Innovation, Denver, CO).

FRAP analysis

GFP-actin was expressed in the testis by crossing the three driver *Drosophila* stock pCOG-GAL4; NGT40; nanos-GAL4 with a pUASpGFP-actin *Drosophila* stock. Similar to the female germline, UAS transgenes are poorly expressed in the male germline. We tried numerous combinations of drivers and targets that were not expressed at high enough levels, especially late in spermatogenesis, for our purpose. Sufficient GFP-actin expression for these experiments was achieved using the three drivers pCOG-GAL4; NGT40; nanos-GAL-4, and a pUASp-GFP-actin transgenic line. The pUASp-vector was originally engineered for enhanced gene expression in female germline (Rørth, 1998). In this combination, a large amount of GFP-actin expression was observed in germline cells at early stages at the apical end of testis. Lower levels were observed at later stages, including during individualization. We compared three combinations of driver and targets: (1) pCOG-GAL4; NGT40; nanos-GAL-4>pUASp-GFP-actin; (2) NGT40; nanos-GAL-4>pUASp-GFP-actin; (3) nanos-GAL-4>pUASp-GFP-actin, and found that the fluorescence of GFP-actin is dependent on the number of drivers. The pUASp-GFP-actin transgene provided more expression when compared with a pUASt-GFP-actin line with the same drivers.

The cysts from male progeny were collected as described above, and transferred to glass bottom dishes (World Precision Instruments inc., Sarasota, FL) coated with poly-L-lysine (Sigma diagnostics, St Louis, MO). Photobleach and subsequent time-lapse imaging were performed using a confocal microscope (TCS SP2, Leica, Iena, Germany) equipped with a 488 nm laser line and 40× and 60× HCX-plan-apo oil immersion lenses. Recovery of fluorescent intensity in the region of interest was measured using Photoshop and plotted using Microsoft Excel. In each experiment FRAP of 5-10 samples was performed.

Membrane labeling in vitro

Membrane dynamics in cystic bulges were examined by labeling cell membrane with 0.5 μM FM 1-43 (Molecular Probes) (Kuromi and Kidokoro, 1998) for 10 minutes. After two washes with culture media, cysts were transferred to a glass bottom dish and examined using confocal microscopy. In the case of double imaging of membrane and GFP-actin, both fluorochromes were excited by 488 nm laser line and detected separately by two barrier filters (500-580 nm for GFP-actin and 600-700 nm for FM1-43). Because FM1-43 has a wide range of emission, barrier filter 500-580 nm passes some of the FM1-43 signal; therefore, membrane is visible in the GFP-actin image. Membrane staining is represented as yellow and GFP-actin is green in the merged image (see Results).

RESULTS

In vitro culture of isolated cysts

We have isolated and cultured individualizing spermatid cysts. Adult testis includes cysts at all stages of spermatogenesis displayed along a developmental gradient. The earliest germ stem cells are located at the apical end of the testis, while later stages, including the elongated cysts that are undergoing individualization are in the basal two thirds of the testis (Fig. 2A) (Fuller, 1993). This makes isolation of elongated cysts straightforward, and enabled us to isolate early spermatocytes and late elongated cysts separately. In the cultures, cysts undergoing individualization could be found for at least 2 days after isolation. Individualizing cysts were easy to identify because they have the characteristic ‘cystic bulge’ somewhere

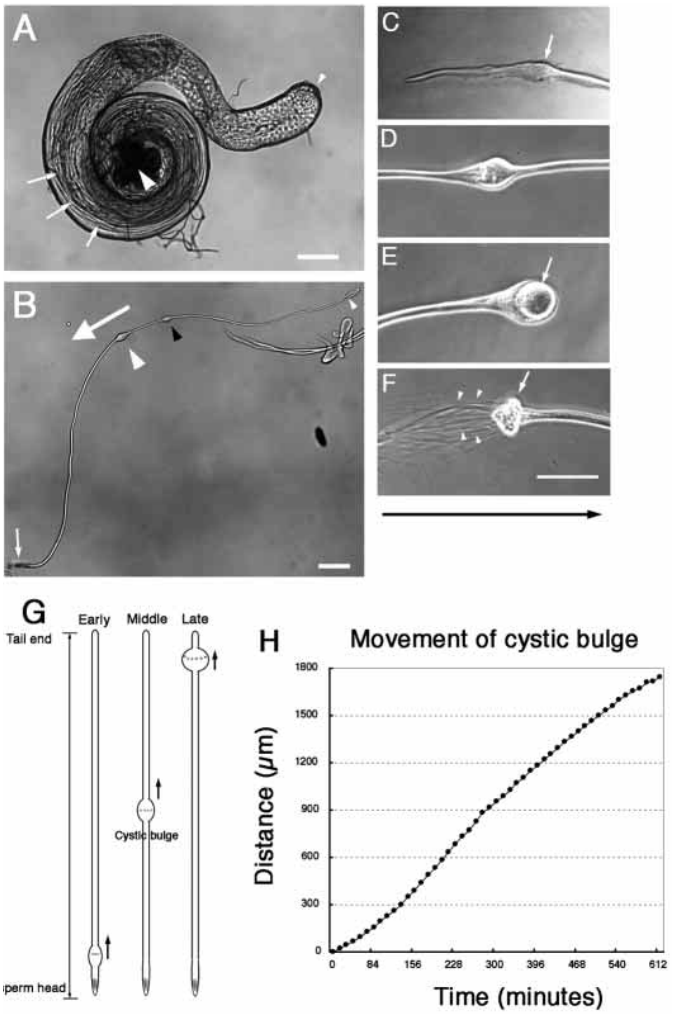

Fig. 2. Primary culture of isolated cyst from *Drosophila* testis. (A) DIC image of dissected testis. Large arrowhead indicates basal (seminal vesicle) end of testis. Fibers (arrows) are elongated cysts. At the apical end (small arrowhead), a number of round cells are seen which are spermatocytes and spermatids at early stages. (B) Isolated individualizing cyst. Large white arrowhead indicates a moving cystic bulge. Large arrow indicates the direction of movement. The cystic bulge starts from the end with sperm nuclei (small white arrowhead) and moves to the apical end (end of sperm tail, small arrow). Small black arrowhead indicates the nuclei of somatic cyst cells, which surround the cyst. (C-F) Cystic bulge at various stages of individualization. The arrow at the bottom indicates the direction of movement of the cystic bulge. (C) Early cystic bulge right after onset of movement (arrow). (D) Cystic bulge in the middle of cyst. (E) Cystic bulge at tail end of cyst. Round waste bag can be seen (arrow). (F) Individualizing spermatids with cyst cells removed. The individualized region of a number of thin sperm tails (small arrowheads) are visible adjacent to the cystic bulge (arrow). (G) An isolated cyst undergoing individualization from head to tail. (H) Representative plot of movement of the cystic bulge. Scale bars: 100 μm in A,B; in F, 50 μm for C-F.

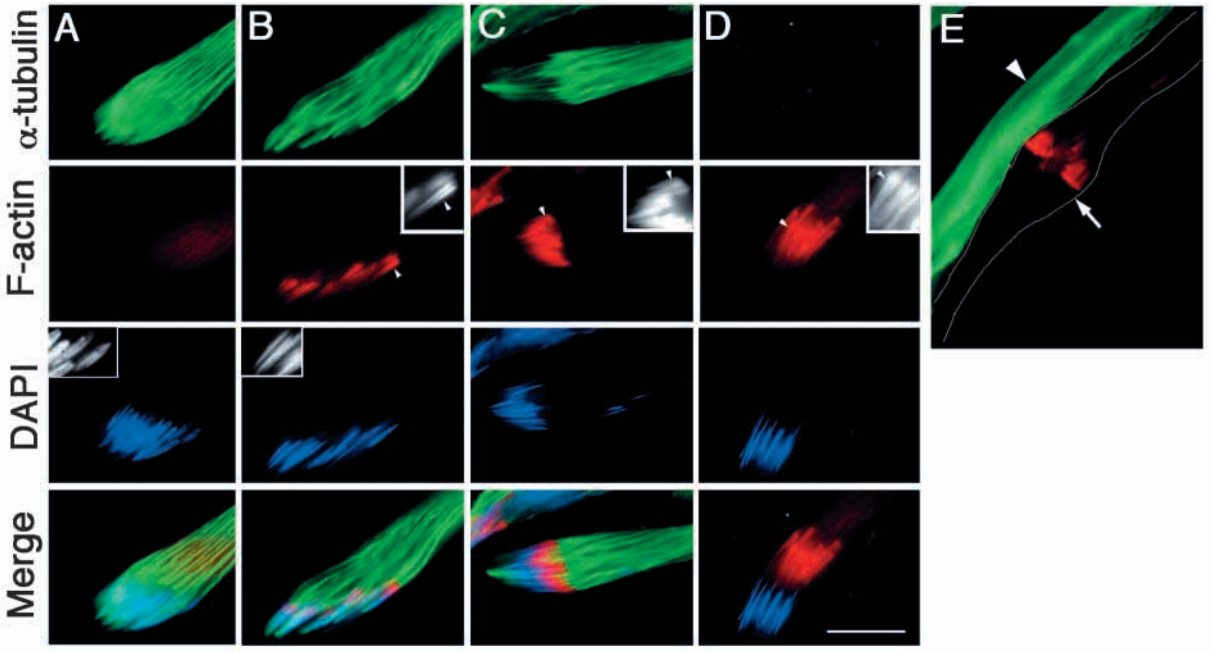

Fig. 3. Immunofluorescence localization of microtubules (green), F-actin (red) and sperm nuclei (blue) in cysts at various stages after elongation. (Column A) Elongated cyst before DNA condensation. There were a number of microtubules around sperm nuclei and microtubule bundles along sperm tails. Nuclei were elongated but not yet condensed (inset). Note that at this stage, no accumulation of actin was seen. (Column B) DNA condensation and F-actin accumulation into an actin cone. Sperm nuclei became thinner (inset in DNA) and actin began to accumulate at the apical side of nuclei. Actin cones were still thin (arrowheads in B-D indicate a single actin cone shown in each inset at higher magnification). (Column C) As the actin cones grew and became thicker, microtubules were excluded from the region but still remained in the cytoplasm. Condensation of sperm nuclei was completed. (Column D) After the onset of actin cone movement, microtubules disappeared. Actin cones became triangular in shape and moved away from the group of sperm nuclei. (E) Actin cones (red) in a cystic bulge in the middle of a cyst. Outline of the individualizing cyst is traced with a white line. The front of the actin cones are wider and the cones are more polarized than at earlier stages. In a non-individualizing cyst (arrowhead), a strong signal of α-tubulin staining (green) was observed. However, the individualizing cyst (arrow) had no α-tubulin signal. Scale bar: 20 μm.

in the middle and the basal side of the cyst is thinner than the apical side (Fig. 2B,D). To observe the whole process of individualization, we identified fully elongated cysts that had not yet begun individualization (i.e. with no cystic bulge and uniform in width all along the length). We observed such cysts from prior to the beginning of individualization until individualization was complete, over the course of 12 hours, using transmitted light microscopy (see Movie 1 at http://dev.biologists.org/supplemental/). Before we saw evidence of individualization, cysts spent several hours without apparent change at the level of our observation. Presumably these cysts were in the process of DNA condensation and maturation of the actin cones. The onset of individualization complex movement was marked by a ruffling of membrane around the sperm head. Once movement began, a cystic bulge formed (Fig. 2). The cystic bulge was small and had a thin spindle shape initially (Fig. 2C). As individualization progressed, the cystic bulge grew bigger (Fig. 2D), eventually becoming round in shape (Fig. 2E). This round structure is the waste bag, which contains all the discarded cytoplasm and vesicles of the syncytial spermatids. After the completion of individualization, the waste bag fell off of the bundle of axonemes. The movement of the cystic bulge was very constant in speed along the cyst (Fig. 2H), although it was slightly slower at both ends. Individualization was completed in about 10 hours and the mean speed of cystic bulge movement was 3 μm/minute. This speed is faster than estimated speed using fixed samples (24 hours for completion) (Tokuyasu et al., 1972), and matches very well with the speed of locomoting cells or *Listeria* movement (1.5-4.0 μm/minute) (Bear et al., 2002; Watanabe and Mitchison, 2002), but is more than six times slower than that of typical unconventional myosins in vitro. Sometimes, during cyst isolation, the somatic cyst cells surrounding syncytial spermatids fell off. This might happen because one of the two cyst cells, called the head-cyst cell, which attaches to the epithelial cell at the basal end of the testis, was removed mechanically during the process of isolation. However, individualization continued normally without the cyst cells. Such syncytial spermatids formed cystic bulges that moved at normal speed and accomplished individualization. In this case, the thin sperm tails of already individualized regions were easily seen sticking out from the cystic bulge (Fig. 2F; see Movie 2 at http://dev.biologists.org/supplemental/). Using this culturing technique both with intact cysts and those without somatic cyst cells, we were able to follow the complete process of individualization with high resolution optics.

Microtubule distribution and nuclear condensation during formation and movement of actin cones

To understand individualization, the mechanism of cystic bulge movement must be defined. Force generation that powers most known processes of cell motility is dependent on the dynamics

of the cytoskeleton and interaction of cytoskeletal proteins with motor proteins. Therefore, we were interested in distributions of cytoskeletal structures that might be important for force generation during movement of the cystic bulge. Previous ultrastructural observations (Tokuyasu, 1974; Tokuyasu et al., 1972) demonstrated that during and after elongation, there are a number of cytoplasmic microtubules along the spermatid that are assumed to be required for nuclear deformation and elongation of spermatids and mitochondrial derivatives (Hoyle and Raff, 1990; Kemphues et al., 1982). The axoneme assembles during elongation. The other major cytoskeletal structures previously described are the actin cones that comprise the individualization complex (Fabrizio et al., 1998; Hicks et al., 1999). However, there has been no systematic description of microtubule and F-actin distribution that would permit correlation of the timing of the changes in distribution with the events of individualization. Therefore, distribution of microtubule structures and F-actin structures was examined at the different stages of individualization by immunofluorescence staining of α-tubulin, F-actin and DNA.

In elongated cysts, prior to the onset of individualization, sperm nuclei were elongated but the DNA was not initially condensed. At this stage, cytoplasmic microtubules were observed running along the length of the spermatids and surrounding the nuclei (Fig. 3A). Actin was not yet accumulated around the apical side of sperm nuclei. After nuclear condensation initiated, F-actin began to accumulate at the basal apical side of nuclei slightly overlapping with them (Fig. 3B). At this stage, a number of cytoplasmic microtubules were still apparent. As the actin continued to accumulate, it became thicker and more triangular in shape, appearing more polarized (Fig. 3C). At this time point, sperm nuclei had completed condensation and microtubules were absent from the region surrounding the nuclei and in the actin accumulations. At the onset of actin cone movement, suddenly microtubule staining disappeared completely throughout the whole cyst (Fig. 3D,E). There is an obvious correlation between the disappearance of cytoplasmic microtubules and onset of actin cone movement (88 out of 89 cysts with actin cones that had not yet moved showed microtubule staining; 61 out of 61 cysts with moving actin cones showed no microtubule staining). Nocodazole treatment disrupted fibrous cytoplasmic microtubule structures, but strong diffuse staining of tubulin remained in the cytoplasm (not shown). However, the fluorescence intensity of diffuse cytoplasmic tubulin staining dropped significantly after the onset of actin cone movement, suggesting that the epitope itself has disappeared. EM observations also failed to detect cytoplasmic microtubules during individualization (Tokuyasu, 1974; Tokuyasu et al., 1972). These results suggest that loss of tubulin staining is not a result of depolymerization, but of destruction of tubulin or modification of C-terminal end of depolymerized α-tubulin. In this stage axoneme tubulin cannot to be seen because the antibody epitope is blocked by modification of the C-terminal end of α-tubulin (Bré et al., 1996). After the onset of movement, actin cones became more triangular. There were no other major actin or microtubule structures visible.

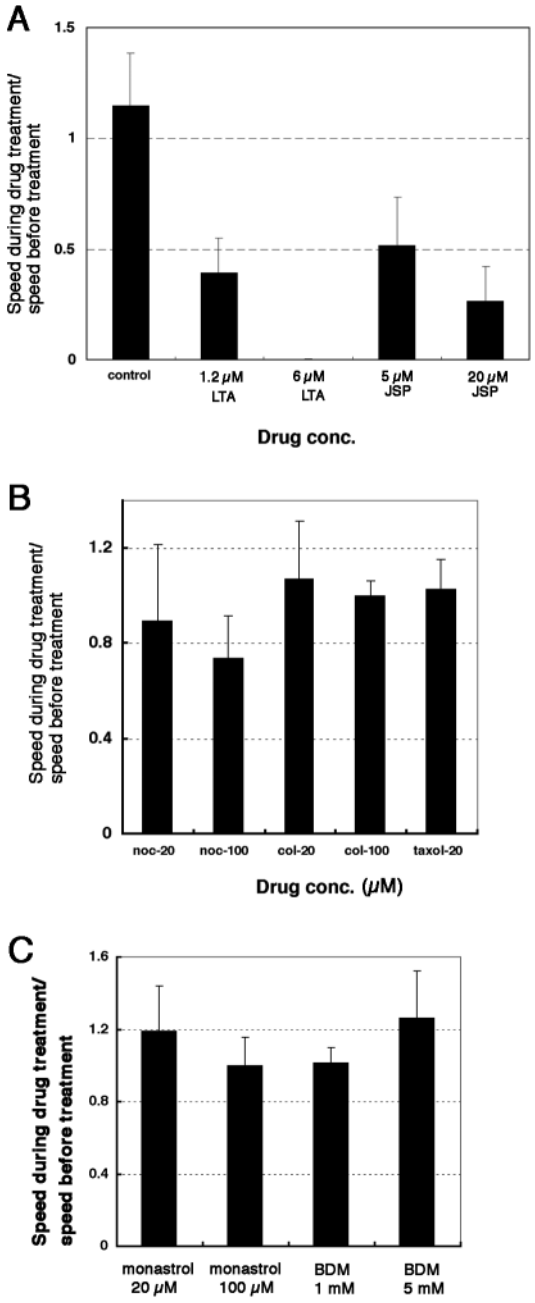

Fig. 4. Effects of pharmacological reagents on cystic bulge movement. Speed before treatment is the average speed of cystic bulge movement for 40 minutes before treatment. Speed during treatment is the average speed from 40 minutes to 80 minutes after application of drug in the same cyst. In each column, average speeds of 5-10 cysts are shown. (A) Effects of drugs that alter actin dynamics. Both LTA and jasplakinolide (JSP) inhibited cystic bulge movement in a dose-dependent manner. LTA (6 μM) completely stopped movement 20 minutes after application. (B) Effects of drugs that alter microtubule dynamics. Nocodazole (noc), colchicine (col) and taxol show minimal effect on cystic bulge movement. (C) Effect of inhibitors of motor proteins. Kinesin inhibitor monastrol and myosin inhibitor BDM did not inhibit movement of the cystic bulge.

Movement of the cystic bulge is actin cytoskeleton dependent

To investigate the motive force of cystic bulge movement, we treated cultured cysts with various cytoskeletal protein inhibitors (Fig. 4). In all experiments with inhibitors, we compared the speed of cystic bulge movement before and after treatment. First, we examined the effect of disrupting actin

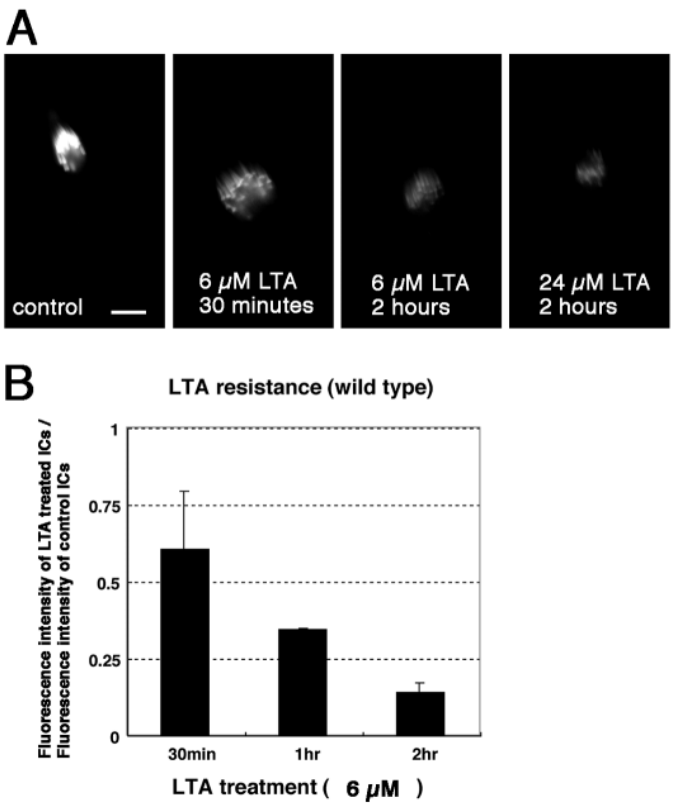

Fig. 5. Actin cones are stable structures. (A) A series of F-actin stainings after LTA treatments of different time duration. Even after 2 hours treatment, some actin cones remained visible. Scale bar: 10 μm. (B) Quantification of fluorescence intensity of individualization complex (IC; a cluster of 64 actin cones in a cystic bulge) after LTA treatment. In order to quantify the effect of treatments, fluorescence intensity of each IC was measured. In each of three experiments and at each time period of treatment, fluorescence intensities of 40 to 50 ICs were measured and average intensities were calculated.

dynamics (Fig. 4A). LTA, an inhibitor of actin polymerization, immediately inhibited cystic bulge movement in a dose-dependent manner. LTA (6 μM) is the typical concentration of this drug used to disrupt actin organization significantly in a wide variety of cell types (Keller, 2000; Tilney et al., 2000; Townsley and Bienz, 2000). At this concentration, cystic bulge movement slowed down immediately after application and stopped completely in about 20 minutes. Jasplakinolide, a cell permeant F-actin stabilizing drug (Bubb et al., 2000; Tilney et al., 2000), also affected movement, although the effect was more subtle. At a concentration of 20 μM, some slow movement was still detected. This concentration is sufficient to disrupt actin-based cell protrusion in locomoting cells and induce abnormal actin organization in fibroblasts (Cramer, 1999). Our results demonstrate that interfering with normal actin dynamics, either by inhibiting assembly or depolymerization caused changes in cystic bulge movement. Interestingly, despite the need for actin polymerization and depolymerization for movement, which would suggest rapid filament turnover, the actin cones of individualization complexes are very stable (Fig. 5). Long incubation (greater than 2 hours) with the actin depolymerizing drug LTA did not completely depolymerize them.

As cytoplasmic microtubules were absent, it seemed unlikely that microtubule-based motility would be involved. However, to rule this out further, we also tested for effects of drugs that affect microtubule dynamics (Fig. 4B). Microtubule destabilizing drugs, colchicine and nocodazole, and a microtubule stabilizing drug, taxol, had no significant effect on movement. The concentrations of each drugs used were very high, and would completely disrupt cytoplasmic microtubules in typical cells (Abe and Uno, 1984; Tilney et al., 2000). We observed that these microtubule drugs were effective in disrupting cytoplasmic microtubules of elongated cysts in earlier stages

Although the above result suggests that microtubules are not required for movement, it remains possible that a motor, like kinesin, might attach to the actin cone and slide along the axoneme in the plus-end direction (Gibbons, 1981). Axonemal microtubules are not likely to be affected by these drug incubations because of their stability. This idea is supported by the fact that there was no shortening of the cyst when treated with microtubule depolymerization drugs (not shown). The other type of microtubule motor, dynein, is unlikely to be involved because it is minus-end directed motor. Therefore, we applied monastrol, a kinesin inhibitor (Fig. 4C) that affects mitotic kinesins. Monastrol did not inhibit movement even at a concentration of 100 μM, a concentration that completely inhibits spindle formation in dividing cells (Mayer et al., 1999). Taken together, our results provide no support for microtubule-based motility processes being important for cystic bulge movement.

Although we have already shown that actin dynamics are important for movement, we wondered whether myosin-based movement might also be important. To test for actin-based motor activity, we used a general myosin ATPase inhibitor, BDM (Cramer and Mitchison, 1995). This drug also did not inhibit movement even at an extremely high concentration (Fig. 4C). These results suggest that some classes of myosins (at least myosin I, II and V) are not directly involved in force generation.

Actin dynamics in actin cone

The above results suggest that actin polymerization is the driving force of cystic bulge movement, as is the case for leading edge protrusion in locomoting cells (Small et al., 2002; Welch and Mullins, 2002). We investigated the similarity of actin dynamics in actin cones to actin structures at the leading edge of moving cells. We asked three main questions:

(1) How quickly does the actin turn over? In lamellipodia, the actin network that drives protrusion turns over very quickly (within 1-2 minutes).

(2) Where are the sites of actin polymerization and depolymerization? It has been shown that polymerization at the membrane and depolymerization away from the leading edge is important for protrusion.

(3) Is there any difference in actin dynamics before and after the onset of actin cone movement? If actin dynamics are important for movement we would expect changes when movement begins.

We investigated actin dynamics in the cones by FRAP using GFP-actin. The maximum expression level of GFP-actin we were able to induce in late cysts, was relatively low (see Materials and Methods). However, the amount of GFP-actin

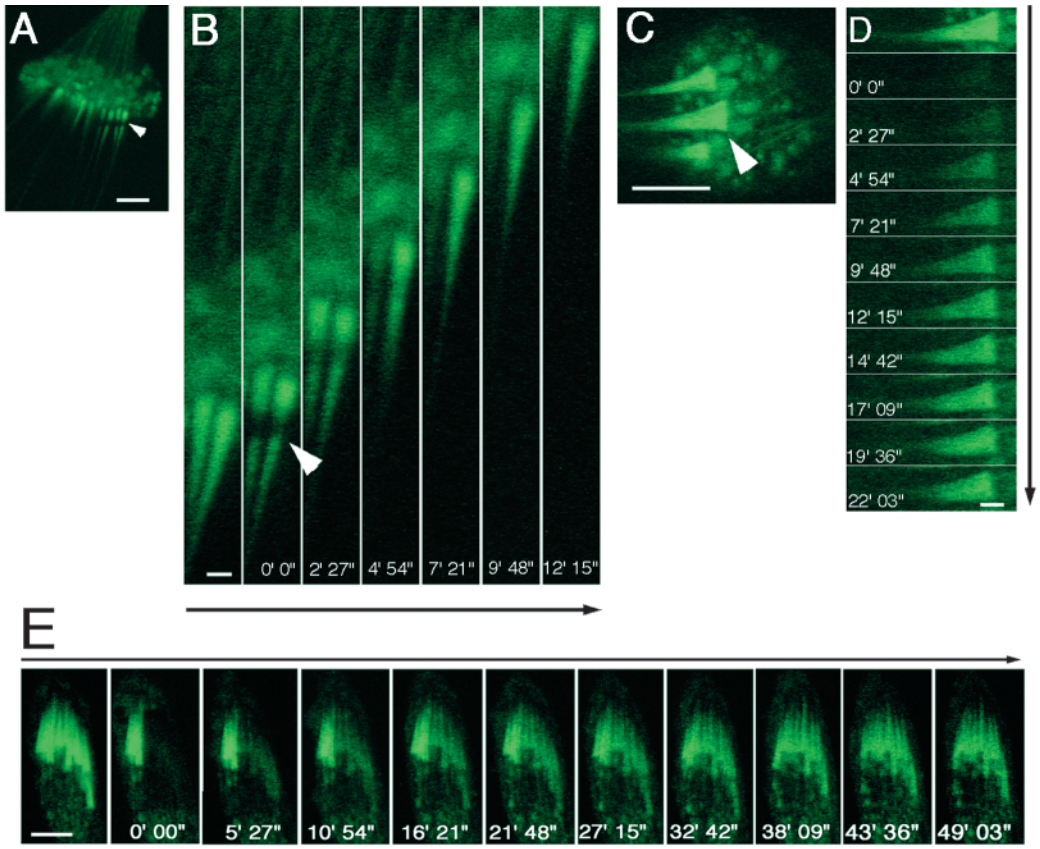

Fig. 6. FRAP of F-actin in cones to examine actin dynamics. (A,B) FRAP experiment 1. Line bleaching across actin cones in a moving cystic bulge. (A) Live image of a moving cystic bulge from a GFP-actin expressing cyst. Arrowhead indicates position of the bleached actin cones. (B) Time-lapse recording of fluorescence recovery after photobleach across a single actin cone. The cystic bulge moved from the bottom to the top of the photograph. Arrowhead indicates position of photobleach. The numbers indicate time after photobleach. Fluorescence recovered completely between 7 minutes 21 seconds and 9 minutes 48 seconds time-points. The bleached spot moved forward as the actin cone moved forward. (C,D) FRAP experiment 2. Bleaching and recovery in a whole single actin cone. (C) Actin cones in moving cystic bulge. Arrowhead indicates actin cone to be bleached. (D) Time series of photobleach and recovery of a whole single actin cone. Recovery takes place relatively uniformly along the cone, and plateaued after 17 minutes 9 seconds, although the fluorescence intensity did not recover completely. (E) FRAP experiment 3. Time series of bleaching and recovery in very early actin cones before onset of movement. Half of the actin cone cluster was bleached. The fluorescence intensity plateaued after 43 minutes 36 seconds. Scale bars: 10 μm for A,C,E; 2.5 μm for B,D.

was sufficient to permit us to perform FRAP experiments. The expression of GFP-actin did not affect cystic bulge movement (2.8±0.2 μm/minute, n=6).

Two different types of FRAP experiments were performed (Figs 6, 7; see Movies 3, 4 at http://dev.biologists.org/supplemental/). First, fluorescence of GFP-actin in moving actin cones was bleached along a line across actin cones, and fluorescent recovery was monitored. A bleached region at any point along the cone completely recovered, indicating that actin turns over everywhere in the actin cone. The bleached line moved forward with the actin cones, suggesting net movement of actin filaments as the actin cone moved (n=7; Fig. 6A,B; Fig. 7A,B). We did not detect a flow of actin from front to back of the actin cone (i.e. treadmilling). This was somewhat surprising and different from leading edge protrusion. Next, fluorescence of a whole single actin cone was bleached (Fig. 6D). We plotted the recovery of fluorescence intensities at the front and the back of the actin cone separately (Fig. 7C,D). Although recovery occurred everywhere, the recovery was quicker in the front. Time for recovery to one half relative intensity at the front was 4 minutes, while at the back, it was 6 minutes (n=6). This suggests that the front of the cone has a slightly more rapid rate of polymerization. In moving actin cones, the actin turned over completely within about 12 minutes.

We also measured turnover in actin cones before onset of movement. It took about 15 minutes to recover to one half relative intensity and recovery plateaued after 40-50 minutes. This slower rate of recovery when compared with moving cones suggests that actin dynamics are highly accelerated after the onset of movement.

Membrane dynamics of cystic bulge

The cystic bulge is the place where membrane remodeling occurs. In previous ultrastructural work, Tokuyasu and colleagues (Tokuyasu et al., 1972) observed a large amount of membranous material in the cystic bulge. In order to reveal membrane structures in the cystic bulge and membrane surrounding the actin cone, we labeled cell membranes using the fluorescent membrane dye, FM 1-43 (Fig. 8), which has been extensively used for probing membrane recycling activity in various cell types (Kuromi and Kidokoro, 1998). This labeling worked best on spermatids where the cyst cells were removed, so that the dye could interact with membrane of the spermatids directly. A solution of 0.5 μM of FM1-43 labels the plasma membrane of the cystic bulge completely within 10 minutes. The membrane forms complex architecture inside the bulge. Optical sectioning demonstrates that these structures are invaginations of plasma membrane with open connections to the outside. These invaginations were present before individualization began. The individualized part of sperm tails directly protruded from the cystic bulge and had no connection with inner membrane structures within the bulge. After incubation with FM 1-43 for 20 minutes and washing, cystic

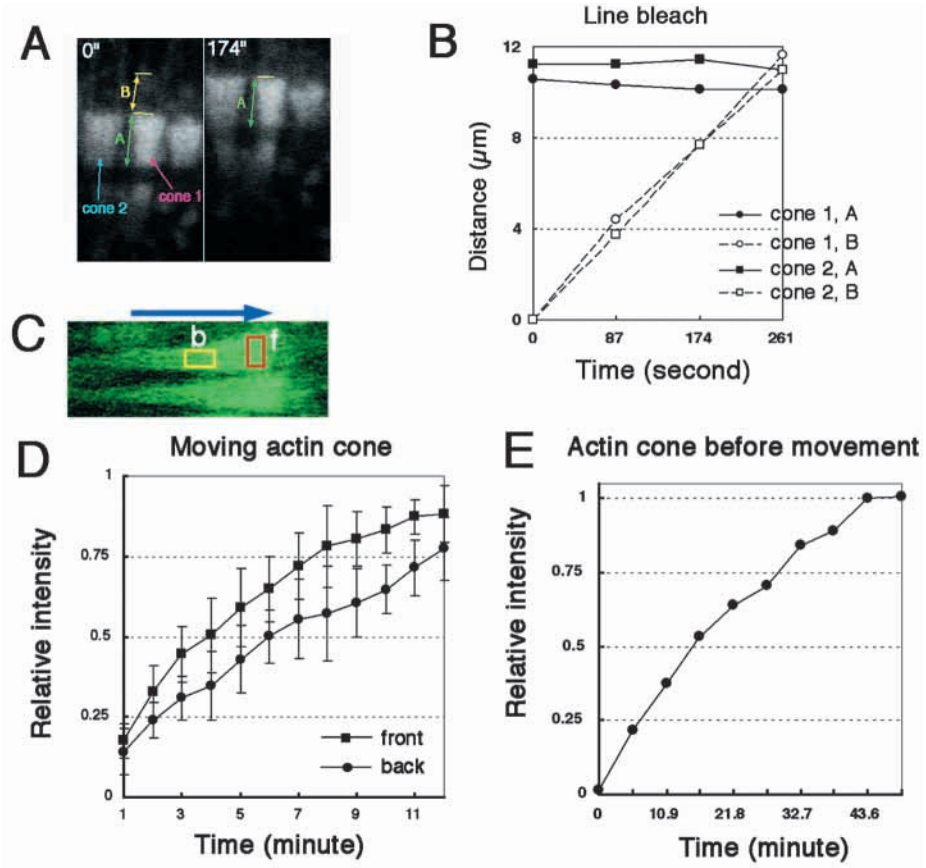

Fig. 7. Plot of fluorescence intensities after photobleach. (A) Raw images of actin cones in a line bleach experiment. The data were used in the plot (B). Numbers in the upper-left corner indicate time after line bleach. Distance A (between green arrowheads) indicates distance from the front of actin cone to the front of bleached line. Distance B (between yellow arrowheads) is the distance of actin cone movement during the time indicated. Short yellow lines indicate the position of front of actin cone in each image. (B) Distances A and B of cone 1 and 2 in A are plotted. Distance A in cone 1 (black circle) and cone 2 (black square) did not change through the recording time suggesting no movement of bleached line relative to the front of the actin cone. However, distance B of cone 1 (white circle) and cone 2 (white square) increased linearly, suggesting constant movement of both actin cones. (C) Representative image of moving actin cones. Fluorescence intensity in the region indicated by rectangles (red:front and yellow:back) were measured and plotted in D. (D) Relative fluorescence intensities of GFP-actin in moving actin cones after photobleaching are plotted. A whole actin cone was photobleached and fluorescence recovery in front (black square) and back (black circle) were plotted separately. Relative intensity was calculated as fluorescence intensity at each time point/fluorescence intensity before photobleach in the region of interest. Six actin cones were examined for each plot. Bulk fluorescence of the actin cone recovers in about 12 minutes in both parts of the cone; however, the front of the cone recovers slightly more quickly than the back. (E) Representative plot of FRAP in actin cones before onset of movement. The fluorescence recovery plataued at 43.6 minutes after photobleach.

bulge movement was observed over a period of 10 minutes. Because the magnification we used was high enough to identify single membrane vesicles, we would expect to see membrane vesicle uptake if there is endocytic activity. However, we could not see any membrane uptake around site of membrane remodeling. Moreover, very few stained membrane vesicles accumulate inside the cystic bulge after incubation with dye (see Movies 5-7 at http://dev.biologists.org/supplemental/). In addition, if exocytosis contributes in a major way to membrane remodeling at this site, we would expect to see appearance of unlabeled membrane patches in the region of the actin cones during the observations made after washing out the dye. These unlabeled regions would be derived from fusion of unlabeled internal membrane vesicles. However, for the entire length of the observation (at 15 second intervals, over 7 minutes), the membrane around the neck looked very flat and homogenous (see Movie 7 at http://dev.biologists.org/supplemental/). Although we did not detect exocytic or endocytic activity in the region of the cystic bulge, we were able to easily detect membrane uptake in the cyst cells surrounding other cysts (see Movie 8 at http://dev.biologists.org/supplemental/) in the same culture. Double imaging of GFP-actin and FM 1-43 revealed that the actin cones localized to the neck of the individualized sperm tail, at the position where the membrane is deformed into thin tubes.

To block endocytosis we raised cysts from mutant flies carrying temperature sensitive allele of dynamin (*shibire*^{1}) (van der Bliek and Meyerowitz, 1991) to the non-permissive temperature. Again, cystic bulge movements were normal [speed at nonpermissive temperature (30°C)/speed at permissive temperature (24°C): *shibire*^{1}=1.6±0.2, *n*=6; weight wild type=1.5±0.3, *n*=5]. In addition, we treated individualizing cysts with the exocytosis inhibitor, BFA (Hendricks et al., 1992; Misumi et al., 1986). This treatment had no effect on movement (speed in the presence of 50 μM BFA/speed before application=1.1±0.2, *n*=5), even after long periods of drug treatment. These results suggest that conventional endocytosis and exocytosis are not likely to play a major part in membrane remodeling around the actin cones.

DISCUSSION

In this report, we observed the whole process of individualization in vitro and have demonstrated that actin polymerization is required for cystic bulge movement. However, this actin-based movement differs in several ways from other previously studied processes, such as *Listeria* motility or leading edge protrusion (see below). In addition, despite the massive remodeling of the membrane that occurs, we found no evidence of endo- or exocytosis at the cystic bulge.

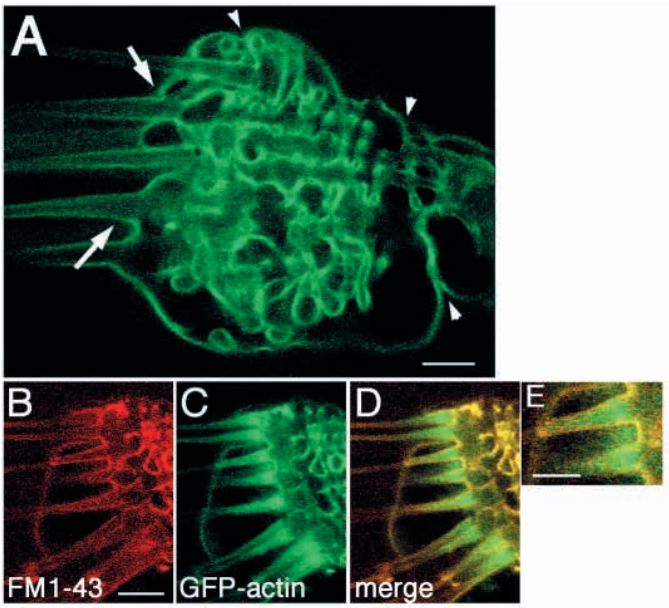

Fig. 8. (A) Live imaging of cell membrane of the cystic bulge with FM1-43. Some open mouths of the membrane tunnels (arrowheads) are indicated. However, around the neck of individualizing sperm tail (arrows), no membrane invaginations or up-take of membrane vesicles was observed. (B-E) Double labeling of membrane with FM 1-43 (B) and F-actin cones with GFP-actin (C). Merged image (D) and higher magnification image (E) demonstrate that F-actin occupied the space of the sperm tail neck that is directly adjacent to the cystic bulge membrane. Scale bars: 6 μm in A,E; in B, 12 μm for B-D.

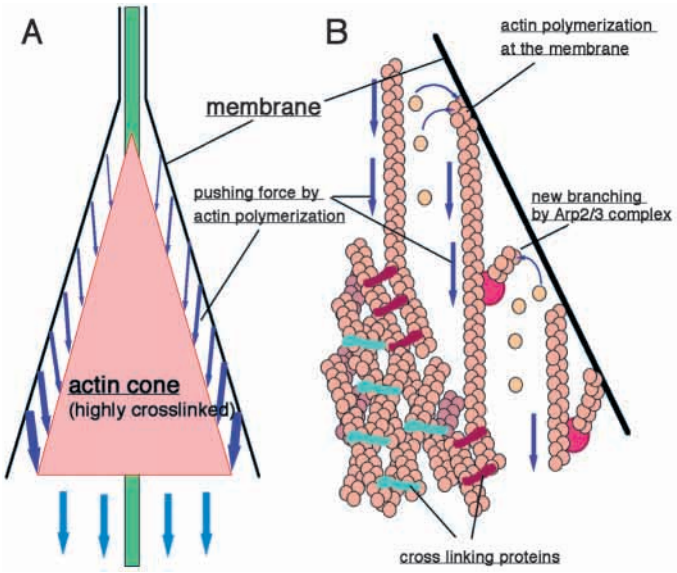

Fig. 9. Model of cystic bulge movement. (A) An actin cone has two domains. The first domain is actin cone itself, which is highly crosslinked and moves forward as a unit. The second domain is cortical actin, which is dynamic and responsible for pushing actin cone forward, as indicated by purple arrows. As the actin cone moves forward (blue arrows), cytoplasm (green) is squeezed out by the thick network in the actin cone. The membrane and axoneme (green bar) become directly connected just behind the actin cone (see the Movie 9 at http://dev.biologists.org/supplemental/). (B) Enlarged diagram of the region of the actin cones and a speculative model of actin dynamics. Actin polymerization occurs near the membrane. The actin filaments elongate and are crosslinked into an actin cone. New filaments branch out from the side the of old filaments due to the activity of Arp2/3 complex. This branching is more active at the front of the actin cone because of the concentration of Arp2/3 complex, and more pushing force should be generated there. Probably because actin depolymerization is faster at the back (and/or there is less assembly), the actin cone becomes thinner toward the back and eventually disappears.

The driving force of movement

Our data are most consistent with the idea that actin cone movement is driven by actin polymerization, similar to lamellipodia extension and *Listeria* motility. The speed of the cystic bulge movement is similar to the speed of movement of the leading edge of lamellipodia (Bear et al., 2002; Watanabe and Mitchison, 2002). Cystic bulge movement is altered very quickly after inhibiting either assembly or disassembly of actin, consistent with the requirement for active actin assembly and disassembly for movement. In FRAP experiments, we detected a slightly faster rate of turnover at the front than in the rear of the cone. It is likely that the faster dynamics of actin at the front is important for movement. In addition, the observed acceleration of actin dynamics after the onset of movement supports this idea. Arp 2/3 complex (Mullins et al., 1998; Welch et al., 1997b), which is the key factor involved in promoting actin polymerization at the leading edge (Welch et al., 1997a), is enriched at the front of actin cones, suggesting that this site is important for force generation. All these data support the idea that the driving force is actin polymerization.

However, some puzzling differences in actin behavior in this structure when compared with leading edge protrusion make it difficult to explain how assembly drives movement in this case. First, we had expected that actin would treadmill through the actin cone from front to back, because of assembly at the front, i.e. in the direction of movement. This has been observed in other actin motility processes. However, this is not the case in actin cones. The filaments in the cone move forward relative to the substrate. Second, actin turns over at a rate that is much slower than that of actin in lamellipodia and *Listeria* comet tails. In both of these structures, filaments turn over in 1-2 minutes (Theriot and Mitchison, 1991; Theriot et al., 1992), but in case of actin cones, turnover takes 12 minutes. Another puzzle is the stability of actin cones to depolymerization by LTA. Actin completely turns over in 12 minutes in moving cones, so we might expect that LTA would cause depolymerization in that time frame. However, even after 2 hours of LTA treatment, cones remain. It is likely that actin in cones is stabilized by binding of cross linkers or other proteins, but the mechanism that regulates stability to permit turnover as the cones move, but prevents depolymerization when assembly stops is not clear.

Despite these differences from other motility processes, our favored model involves only actin assembly as the driving force for motility. In order to explain the dynamics of actin in the cone and results of pharmacological experiments, we would suggest that there are two actin structural components in a moving actin cone. The first actin structure is the actin cone itself. The three characteristics discussed above (stability, filament translocation and slow turnover) suggest that the actin cone is a highly organized and stable structure compared to the

actin network in lamellipodia. It is likely that each actin cone moves forward as one unit. The second actin structure component is an actin network near the membrane that pushes the actin cone forward by force of polymerization. Actin filaments elongate near the membrane, similar to the leading edge, but the membrane is held rigid, rather than protruding as it does at the leading edge (Fig. 9). In this case, a photobleached GFP-actin in a filament would be pushed away from the membrane, i.e. 'forward' relative to the membrane. Eventually, this filament would be crosslinked into the actin cone as new actin filaments assembled. This model is consistent with our data, but we do not have information about the orientation of actin filaments and the sites of actin monomer incorporation that would provide additional support for such a model. In addition, the molecules that might be important to keep the membrane rigid and prevent its protrusion are as yet unknown.

An alternative model is that myosin based motility contributes to movement by generating force using cortical actin and/or actin cones as a substrate for movement. Using a motor protein to provide force is compatible with the idea that the actin cone moves forward as a unit. However, it is not obvious why motor-driven movement would be coupled with actin dynamics. Perhaps movement requires a dynamic cortical actin network around the actin cone, to provide tracks for myosin movement. This track might need to be continually assembled at new sites during movement. As the actin cone is a very large and intensely labeled structure, it might be hard to detect the different dynamic behavior in a less prominent, thin cortical structure in the same region. Myosin VI is present on actin cones and essential for individualization (Hicks et al., 1999) making it tempting to speculate that myosin VI might provide the driving force. However, cystic bulges of myosin VI mutants can move partway along the cyst (Hicks et al., 1999) (T.N. and K.G.M., unpublished), indicating its function is not required for cone movement. Instead, myosin VI is important for regulating actin dynamics during movement (Rogat and Miller, 2002) (T.N. and K.G.M., unpublished). Other myosins may be important for some aspects of cystic bulge movement, but this remains to be demonstrated. BDM, an inhibitor of myosin ATPases, did not block movement. This inhibitor has been demonstrated to block activity of myosin I, II and V, suggesting it is a general inhibitor (Cramer and Mitchison, 1995). The lack of effect of BDM on cone movement makes a myosin-based motility model less likely, but we cannot definitively rule out all myosins as force generators in this process at this time. Mutant alleles of all the predicted myosins in the *Drosophila* are not available and the effect of BDM on myosins in many classes is unknown.

Microtubule-based motility is not likely to be involved in cone movement. There are no cytoplasmic microtubules, which might participate in generating force in cooperation with microtubule motors and inhibitors of microtubule dynamics, and motors do not stop movement. In addition, when actin dynamics are altered, the cystic bulge stops immediately. If the movement was microtubule based, it is not clear why actin dynamics would be important.

Further studies are required to provide support for our model of actin cone motility. Additional studies examining membrane dynamics, effect of disruption of actin polymerization regulators and ultrastructure of the actin cones will be needed for more insight into the similarities and differences in the mechanism of actin cone movement and lamellipodia extension.

The role of actin cones in individualization

Although we do not yet understand fully the mechanism of actin cone movement, we can speculate about the role of actin cones during individualization. We suggest that the actin cones have three roles (Fig. 9). First, the actin cones have the ability to push the cystic bulge forward, using actin polymerization. Second, the actin cones sweep the cytoplasm and organelles out of the sperm flagella, acting as a sieve. Finally, the actin cones must bind the cell membrane around them and shape it into the observed thin tubular structure. Eventually, as the actin depolymerizes at the cone tip, the membrane must attach to the axoneme.

Microtubule structure and formation of actin cones: signal for a dramatic transition?

There is an interesting transition that occurs as individualization begins. Microtubule staining disappears during a very short period around the onset of actin cone movement. Our data suggests that this disappearance is due to tubulin degradation as movement begins. This idea is supported by previous observations that the amount of tubulin present in individualized spermatids was much less than in cysts prior to individualization (Kemphues et al., 1980), and that cytoplasmic microtubules disappear during individualization (Tokuyasu et al., 1972).

This transition temporally coincides with the onset of actin cone movement, rather than sperm nucleus DNA condensation. FRAP experiments demonstrated that actin dynamics also accelerated after the onset of movement. Therefore, we suspect that a global signal orchestrates these events to trigger the onset of individualization.

Membrane remodeling does not require endocytosis or exocytosis.

Conventional endocytosis may not be important for movement of the cystic bulge, because FM1-43 staining of cell membrane demonstrated that membrane uptake did not take place around the actin cones and blocking endocytosis using temperature shift of the *shibire* (dynamin) mutant did not affect cystic bulge movement. In addition, no concentration of α-adaptin has been observed in the region around the actin cones, suggesting that no coated pit formation occurs there (Rogat and Miller, 2002). Conversely, clathrin mutants have defects in individualization (Bazinet et al., 1993; Fabrizio et al., 1998), but the reason that individualization fails has not been well studied. The discrepancies in these data will only be resolved by further analysis of the clathrin mutant phenotype and studies of the effects of loss of function in other proteins in the endocytosis pathway.

Likewise, exocytosis may not play major role in the membrane remodeling process, because FM1-43 membrane staining suggests that there is not a significant amount of membrane insertion at the sites around the actin cones, and BFA treatment did not affect the movement of cystic bulge. Our data do not completely exclude the possibility that exocytic events participate in remodeling, as we could not directly measure the exocytosis. However, it seems more likely

that the large number of membrane invaginations that are present in the cystic bulge is a sufficient source of membrane to accomplish remodeling. As seen in the movie of FM1-43 labeled spermatids (Movies 6, 7 at http://dev.biologists.org/supplemental/, the plasma membrane seems to be smoothly reorganized into thin tubular structures around the actin cones. Furthermore, ultrastructural observations have shown that the membrane around actin cones (investment cone in their terminology) is flat, without any invaginating or docking membrane vesicles (Tokuyasu et al., 1972) (T.N., unpublished). These data support the idea that the cell membrane in the cystic bulge is directly deformed into a thin tubular structure.

Culturing cysts in vitro

The whole process of spermatogenesis from germ stem cell differentiation to individualization into motile sperm occurs continuously during adult life. There are many processes of interest to cell and developmental biologists that occur during the different stages of spermatid differentiation. These processes include meiosis, cell elongation, membrane remodeling, discarding of cytoplasm and flagella formation. The culture system we have used is suitable for studies in vitro of many aspects of spermatogenesis, as most of the processes are evident in these cultures. Through culturing of testes from various male sterile mutants and ectopically expressing a variety of genes, including GFP-tagged proteins, it should be possible to learn much about these events. Our studies using these cultures have successfully demonstrated that actin polymerization is important for individualization. Studies are in progress to fully understand how actin cones move and how they associate with the membrane.

The authors thank Andy Hudson at Yale University and the Bloomington Stock Center for useful fly lines. We also thank Deborah Frank, Aaron Rogat, Roberta Hopmann and Wei-Lih Lin for valuable discussion and critical reading of this manuscript. This work was supported by a grant from National Institutes of Health to K.G.M.

REFERENCES

Abe, S. and Uno, S. (1984). Nuclear elongation of dissociated newt spermatids in vitro and their nuclear shortening by antimicrotubule agents. *Exp Cell Res* **154**, 243-255.

Bazinet, C., Katzen, A. L., Morgan, M., Mahowald, A. P. and Lemmon, S. K. (1993). The Drosophila clathrin heavy chain gene: clathrin function is essential in a multicellular organism. *Genetics* **134**, 1119-1134.

Bear, J. E., Svitkina, T. M., Krause, M., Schafer, D. A., Loureiro, J. J., Strasser, G. A., Maly, I. V., Chaga, O. Y., Cooper, J. A., Borisy, G. G. et al. (2002). Antagonism between Ena/VASP proteins and actin filament capping regulates fibroblast motility. *Cell* **109**, 509-521.

Bré, M. H., Redeker, V., Quibell, M., Darmanaden-Delorme, J., Bressac, C., Cosson, J., Huitorel, P., Schmitter, J. M., Rossler, J., Johnson, T. et al. (1996). Axonemal tubulin polyglycylation probed with two monoclonal antibodies: widespread evolutionary distribution, appearance during spermatozoan maturation and possible function in motility. *J. Cell Sci.* **109**, 727-738.

Bubb, M. R., Spector, I., Beyer, B. B. and Fosen, K. M. (2000). Effects of jasplakinolide on the kinetics of actin polymerization. An explanation for certain in vivo observations. *J. Biol. Chem.* **275**, 5163-5170.

Castrillon, D. H., Gonczy, P., Alexander, S., Rawson, R., Eberhart, C. G., Viswanathan, S., DiNardo, S. and Wasserman, S. A. (1993). Toward a molecular genetic analysis of spermatogenesis in Drosophila melanogaster: characterization of male-sterile mutants generated by single P element mutagenesis. *Genetics* **135**, 489-505.

Cramer, L. P. (1999). Role of actin-filament disassembly in lamellipodium protrusion in motile cells revealed using the drug jasplakinolide. *Curr. Biol.* **9**, 1095-1105.

Cramer, L. P. and Mitchison, T. J. (1995). Myosin is involved in postmitotic cell spreading. *J. Cell Biol.* **131**, 179-189.

Cross, D. P. and Sang, J. H. (1978). Cell culture of individual Drosophila embryos. I. Development of wild-type cultures. *J. Embryol. Exp. Morphol.* **45**, 161-172.

Cross, D. P. and Shellenbarger, D. L. (1979). The dynamics of Drosophila melanogaster spermatogenesis in in vitro cultures. *J. Embryol. Exp. Morphol.* **53**, 345-351.

Fabrizio, J. J., Hime, G., Lemmon, S. K. and Bazinet, C. (1998). Genetic dissection of sperm individualization in Drosophila melanogaster. *Development* **125**, 1833-1843.

Fowler, G. L. (1973). In vitro cell differentiation in the testes of Drosophila hydei. *Cell Differ.* **2**, 33-42.

Fuller, M. T. (1993). Spermatogenesis. In *The Development of* Drosophila melanogaster (ed. M. Bate and A. M. Arias), pp. 71-147. Cold Spring Harbor, New York: Cold Spring Harbor Laboratory Press.

Fuller, M. T. (1998). Genetic control of cell proliferation and differentiation in Drosophila spermatogenesis. *Semin. Cell Dev. Biol.* **9**, 433-444.

Gibbons, I. R. (1981). Cilia and flagella of eukaryotes. *J. Cell Biol.* **91**, S107-S124.

Gonczy, P., Viswanathan, S. and DiNardo, S. (1992). Probing spermatogenesis in Drosophila with P-element enhancer detectors. *Development* **114**, 89-98.

Hendricks, L. C., McClanahan, S. L., Palade, G. E. and Farquhar, M. G. (1992). Brefeldin A affects early events but does not affect late events along the exocytic pathway in pancreatic acinar cells. *Proc. Natl. Acad. Sci. USA* **89**, 7242-7246.

Hicks, J. L., Deng, W. M., Rogat, A. D., Miller, K. G. and Bownes, M. (1999). Class VI unconventional myosin is required for spermatogenesis in Drosophila. *Mol. Biol. Cell* **10**, 4341-4353.

Hoyle, H. D. and Raff, E. C. (1990). Two Drosophila beta tubulin isoforms are not functionally equivalent. *J. Cell Biol.* **111**, 1009-1026.

Hudson, A. M. and Cooley, L. (2002). A subset of dynamic actin rearrangements in Drosophila requires the Arp2/3 complex. *J. Cell Biol.* **156**, 677-687.

Keller, H. U. (2000). Redundancy of lamellipodia in locomoting Walker carcinosarcoma cells. *Cell Motil. Cytoskel.* **46**, 247-256.

Kemphues, K. J., Kaufman, T. C., Raff, R. A. and Raff, E. C. (1982). The testis-specific beta-tubulin subunit in Drosophila melanogaster has multiple functions in spermatogenesis. *Cell* **31**, 655-670.

Kemphues, K. J., Raff, E. C., Raff, R. A. and Kaufman, T. C. (1980). Mutation in a testis-specific beta-tubulin in Drosophila: analysis of its effects on meiosis and map location of the gene. *Cell* **21**, 445-451.

Kuromi, H. and Kidokoro, Y. (1998). Two distinct pools of synaptic vesicles in single presynaptic boutons in a temperature-sensitive Drosophila mutant, shibire. *Neuron* **20**, 917-925.

Laughran, L. J., Stanley, H. P. and Bowman, J. T. (1976). Electron microscopic study of postcytokinetic cell fusion in an autosomal male sterile mutant (ms(2)3R) of Drosophila melanogaster. *J. Ultrastruct. Res.* **56**, 21-30.

Liebrich, W. (1981). In vitro spermatogenesis in Drosophila. I. Development of isolated spermatocyte cysts from wild-type D. hydei. *Cell Tissue Res.* **220**, 251-262.

Liebrich, W. (1982). The effects of cytochalasin B and colchicine on the morphogenesis of mitochondria in Drosophila hydei during meiosis and early spermiogenesis. An in vitro study. *Cell Tissue Res.* **224**, 161-168.

Lifschytz, E. and Hareven, D. (1977). Gene expression and the control of spermatid morphogenesis in Drosophila melanogaster. *Dev. Biol.* **58**, 276-294.

Lindsley, D. I. and Lifschytz, E. (1972). The genetic control of spermatogenesis in Drosophila. In *The Genetics of Spermatozoon* (ed. R. A. Beatty and S. Gluecksohn-Waelsch), pp. 203-222. Copenhagen: Bogtrykkeriet Forum.

Lindsley, D. I. and Tokuyasu, K. T. (1980). Spermatogenesis. In *Genetics and Biology of* Drosophila, 2nd edn (ed. M. Ashburner and T. R. Wright), pp. 225-294. New York: Academic Press.

Mayer, T. U., Kapoor, T. M., Haggarty, S. J., King, R. W., Schreiber, S. L. and Mitchison, T. J. (1999). Small molecule inhibitor of mitotic spindle bipolarity identified in a phenotype-based screen. *Science* **286**, 971-974.

Misumi, Y., Miki, K., Takatsuki, A., Tamura, G. and Ikehara, Y. (1986). Novel blockade by brefeldin A of intracellular transport of secretory proteins in cultured rat hepatocytes. *J. Biol. Chem.* **261**, 11398-11403.

Mullins, R. D., Heuser, J. A. and Pollard, T. D. (1998). The interaction of

Arp2/3 complex with actin: nucleation, high affinity pointed end capping, and formation of branching networks of filaments. *Proc. Natl. Acad. Sci. USA* **95**, 6181-6186.

Robinson, D. N. and Cooley, L. (1997). Examination of the function of two kelch proteins generated by stop codon suppression. *Development* **124**, 1405-1417.

Rogat, A. D. and Miller, K. G. (2002). A role for myosin VI in actin dynamics at sites of membrane remodeling during *Drosophila* spermatogenesis. *J. Cell Sci.* **115**, 4855-4865.

Romrell, L. J., Stanley, H. P. and Bowman, J. T. (1972). Genetic control of spermiogenesis in Drosophila melanogaster: an autosomal mutant (ms(2)10R) demonstrating disruption of the axonemal complex. *J. Ultrastruct. Res.* **38**, 578-590.

Rørth, P. (1998). Gal4 in the Drosophila female germline. *Mech. Dev.* **78**, 113-118.

Small, J. V., Stradal, T., Vignal, E. and Rottner, K. (2002). The lamellipodium: where motility begins. *Trends Cell Biol.* **12**, 112-120.

Theriot, J. A. and Mitchison, T. J. (1991). Actin microfilament dynamics in locomoting cells. *Nature* **352**, 126-131.

Theriot, J. A., Mitchison, T. J., Tilney, L. G. and Portnoy, D. A. (1992). The rate of actin-based motility of intracellular Listeria monocytogenes equals the rate of actin polymerization. *Nature* **357**, 257-260.

Tilney, L. G., Connelly, P. S., Vranich, K. A., Shaw, M. K. and Guild, G. M. (2000). Actin filaments and microtubules play different roles during bristle elongation in Drosophila. *J. Cell Sci.* **113**, 1255-1265.

Tokuyasu, K. T. (1974). Dynamics of spermiogenesis in Drosophila melanogaster. 3. Relation between axoneme and mitochondrial derivatives. *Exp. Cell Res.* **84**, 239-250.

Tokuyasu, K. T., Peacock, W. J. and Hardy, R. W. (1972). Dynamics of spermiogenesis in Drosophila melanogaster. I. Individualization process. *Z Zellforsch. Mikrosk. Anat.* **124**, 479-506.

Townsley, F. M. and Bienz, M. (2000). Actin-dependent membrane association of a Drosophila epithelial APC protein and its effect on junctional Armadillo. *Curr. Biol.* **10**, 1339-1348.

Tracey, W. D., Jr, Ning, X., Klingler, M., Kramer, S. G. and Gergen, J. P. (2000). Quantitative analysis of gene function in the Drosophila embryo. *Genetics* **154**, 273-284.

van der Bliek, A. M. and Meyerowitz, E. M. (1991). Dynamin-like protein encoded by the Drosophila shibire gene associated with vesicular traffic. *Nature* **351**, 411-414.

Watanabe, N. and Mitchison, T. J. (2002). Single-molecule speckle analysis of actin filament turnover in lamellipodia. *Science* **295**, 1083-1086.

Welch, M. D., DePace, A. H., Verma, S., Iwamatsu, A. and Mitchison, T. J. (1997a). The human Arp2/3 complex is composed of evolutionarily conserved subunits and is localized to cellular regions of dynamic actin filament assembly. *J. Cell Biol.* **138**, 375-384.

Welch, M. D., Iwamatsu, A. and Mitchison, T. J. (1997b). Actin polymerization is induced by Arp2/3 protein complex at the surface of Listeria monocytogenes. *Nature* **385**, 265-269.

Welch, M. D. and Mullins, R. D. (2002). Cellular control of actin nucleation. *Annu. Rev. Cell Dev Biol.* **18**, 247-288.

Wilkinson, R. F., Stanley, H. P. and Bowman, J. T. (1974). Genetic control of spermiogenesis in Drosophila melanogaster: the effects of abnormal cytoplasmic microtubule populations in mutant ms(3)10R and its colcemid-induced phenocopy. *J. Ultrastruct. Res.* **48**, 242-258.